Remote Sensing of Environment 115 (2011) 692–702

Contents lists available at ScienceDirect

Remote Sensing of Environment

journal homepage: www.elsevier.com/locate/rse

Analysis of monotonic greening and browning trends from global NDVI time-series

Rogier de Jong [a,b,*], Sytze de Bruin [a], Allard de Wit [c], Michael E. Schaepman [a,d], David L. Dent [e]

[a] Laboratory of Geo–Information Science and Remote Sensing, Wageningen University, The Netherlands
[b] ISRIC-World Soil Information, Wageningen, The Netherlands
[c] Alterra, Wageningen, The Netherlands
[d] Remote Sensing Laboratories, University of Zurich, Switzerland
[e] Merchants of Light Ltd, Norwich, England, United Kingdom

ARTICLE INFO

Article history:
Received 16 March 2010
Received in revised form 24 September 2010
Accepted 23 October 2010

Keywords:
Global vegetation trends
Phenology
Harmonic analysis
GIMMS NDVI
Seasonal Mann–Kendall

ABSTRACT

Remotely sensed vegetation indices are widely used to detect greening and browning trends; especially the global coverage of time-series normalized difference vegetation index (NDVI) data which are available from 1981. Seasonality and serial auto-correlation in the data have previously been dealt with by integrating the data to annual values; as an alternative to reducing the temporal resolution, we apply harmonic analyses and non-parametric trend tests to the GIMMS NDVI dataset (1981–2006). Using the complete dataset, greening and browning trends were analyzed using a linear model corrected for seasonality by subtracting the seasonal component, and a seasonal non-parametric model. In a third approach, phenological shift and variation in length of growing season were accounted for by analyzing the time-series using vegetation development stages rather than calendar days. Results differed substantially between the models, even though the input data were the same. Prominent regional greening trends identified by several other studies were confirmed but the models were inconsistent in areas with weak trends. The linear model using data corrected for seasonality showed similar trend slopes to those described in previous work using linear models on yearly mean values. The non-parametric models demonstrated the significant influence of variations in phenology; accounting for these variations should yield more robust trend analyses and better understanding of vegetation trends.

1. Introduction

Vegetation, as the main component of the terrestrial biosphere, is a crucial element in the climate system (Foley et al., 2000) and there is high confidence that global warming is now strongly affecting the terrestrial biosphere (IPCC, 2007). Vegetation status is commonly used in assessments of productivity of natural and agricultural lands (Cai & Sharma, 2010; Sims et al., 2008; Yu et al., 2009) and a declining, or *browning*, trend is considered to indicate land degradation (Metternicht et al., 2010; Wessels et al., 2007; Zika & Erb, 2009). Normalized Difference Vegetation Index (NDVI), based on red and near-infrared reflectance (Tucker, 1979), is strongly correlated with vegetation productivity (Prince & Tucker, 1986; Tucker et al., 1985) and trends in NDVI can thus be used as a proxy for greening or browning (Alcaraz-Segura et al., 2009; Bai et al., 2008). However, it is difficult to attribute cause-and-effect to vegetation trends because variations in vegetation productivity are driven by various factors, including climatic cycles and management practices (Evans & Geerken, 2004; Lupo et al., 2001; Wessels et al., 2007).

NDVI trends have been used for many purposes, including assessment of ecological response to global warming (Pettorelli et al., 2005), phenological change (White et al., 2009), crop status (Tottrup & Rasmussen, 2004), land cover change (Hüttich et al., 2007) or desertification (Symeonakis & Drake, 2004). For example, systematic greening has been found in the Sahel (Anyamba & Tucker, 2005; Heumann et al., 2007; Olsson et al., 2005), most likely due to climatic variations and recovery from severe droughts (Herrmann et al., 2005; Nicholson, 2000). The effects of human-induced land degradation are highlighted by some studies (Hein & de Ridder, 2006) and disputed by others (Prince et al., 2007; Seaquist et al., 2008). At the global scale, Bai et al. (2008) combined NDVI trends with rain-use efficiency as a proxy of degradation. Most analyses established trends by linear regression of NDVI, integrated annually (Bai et al., 2008) or seasonally (Eklundh & Olsson, 2003) but it is not always clear whether a fitted slope coefficient differs significantly from zero (de Beurs & Henebry, 2004) or what may be the effect of integration by calendar year in the southern hemisphere where growing seasons straddle the year end (Wessels, 2009).

Trends and inter-annual variability in vegetation phenology – the timing of seasonal activities of plants – affect the exchange of carbon, water and energy between the vegetation and the atmosphere (Baldocchi et al., 2001). A range of studies using station observations

* Corresponding author. P.O. Box 47, 6700 AA Wageningen, The Netherlands. Tel.: +31 317483734; fax: +31 317 419000.
E-mail address: Rogier.deJong@wur.nl (R. de Jong).

0034-4257/$ – see front matter © 2010 Elsevier Inc. All rights reserved.
doi:10.1016/j.rse.2010.10.011

of phenology and temperature has shown a widespread trend of earlier onset of greening and longer growing seasons, especially in the Northern Hemisphere (Menzel et al., 2006; Rosenzweig et al., 2007; Sparks et al., 2009); these findings are substantiated by satellite observations since the early 1980s (Karlsen et al., 2007; Myneni et al., 1997; Tucker et al., 2001; Zhou et al., 2001) and are in line with the increase in net primary production suggested by modeling (Nemani et al., 2003). Longer and warmer growing seasons increase evapotranspiration and drought stress (Barber et al., 2000; Zhang et al., 2009), wildfire incidence (Westerling et al., 2006) and intensity of carbon sequestration (Goulden et al., 1996; White et al., 1999). Therefore, a decrease in the growth rate within the growing season might be a more sensitive measure than total production as an indicator of stress and soil degradation. Unfortunately, information on growth rate, or intensity, is concealed by integration of NDVI data to annual values.

When complete NDVI time-series are analyzed for trends, without temporal integration, linear regression needs to be used with care because any auto-correlation within the dataset will violate some model assumptions (Beck et al., 2006; de Beurs & Henebry, 2004; McBride et al., 1994) and trends may be less significant than they appear. Either seasonality must be removed (Hussian et al., 2005) or a non-parametric trend test that accounts for seasonality may be applied (de Beurs & Henebry, 2004). In the Sahel, growth intensity has been measured by a combination of the seasonal amplitude and the seasonal total but the amplitude appeared to be affected by saturation of the NDVI signal (Eklundh & Olsson, 2003). The non-parametric analysis will not be so affected because NDVI values near the beginning and end of the season are well below saturation level.

This paper considers monotonic trends; accordingly it is assumed that trends preserve their increasing or decreasing order throughout the time-series. We examine differences between previously-published methods using the 1981–2006 Global Inventory Modeling and Mapping Studies (GIMMS) NDVI dataset (Bai & Dent, 2009; Bai et al., 2008) and suggested improvements that do not reduce temporal resolution: 1) a linear model applied to NDVI residuals after the seasonal component has been removed; 2) a non-parametric model applied to the original NDVI data; 3) a non-parametric model applied to vegetation development stages (NDVI data adjusted for the growing season). Long-term and annual harmonic analyses were used to filter cloudiness and seasonality, and to derive phenological measures.

2. Materials and methods

Harmonic analysis was applied to the NDVI data to remove residual cloud and haze effects and seasonality. Greening and browning trends were then investigated using linear and non-parametric models, summarizing the outputs by biome.

2.1. The GIMMS dataset

NDVI is the most-used product derived from the National Oceanographic and Atmospheric Administration (NOAA) Advanced Very High Resolution Radiometer (AVHRR) data (Cracknell, 2001). We used GIMMS version G (Tucker et al., 2004), consisting of 26 years of NDVI data from 1981 through 2006, summarized fortnightly at 8 km resolution. The fortnightly time-series was derived from daily 4 km global area coverage data from a suite of NOAA satellites (Tucker et al., 2005), applying the maximum-value-composite (MVC) technique to remove bias caused by atmospheric conditions (Holben, 1986). However, this is not an atmospheric-correction method and some inaccuracy remains, especially in hazy and cloudy conditions (Nagol et al., 2009). Orbital decay and changes in NOAA satellites are known to affect AVHRR data but processed NDVI data have been found to be free of trends introduced from these effects (Kaufmann et al., 2000). This is confirmed by a study in the Sahel to the effects of shifts in solar zenith angle on NDVI (Eklundh & Olsson, 2003).

2.2. Harmonic analysis of NDVI time-series

Phenological patterns were extracted from the GIMMS data using a modified implementation of the HANTS algorithm (de Wit & Su, 2005; Roerink et al., 2000) which describes seasonal effects in vegetation using a limited number of low-frequency cosine functions with different phases, frequencies and amplitudes. The algorithm uses Fourier analysis, complemented with detection of outliers, which are flagged and replaced iteratively (Fig. 1).

First, the raw GIMMS data are used as input for a fast Fourier transform (FFT). The frequencies representing the yearly, 6-monthly and 4-monthly signals are selected from the Fourier spectrum. Based on these frequencies, the spectrum is transformed back to a filtered NDVI time-series using inverse FFT. Outliers are filtered using a fit-error tolerance (FET): each original NDVI value that deviates from the harmonic curve by more than the FET-value is considered as noise and is replaced by the filtered value. This procedure is repeated until either no points exceed the FET or a pre-defined constraint is reached; the constraints concern the maximum number of iterations (i_{MAX}) or a threshold on retained data points, which is closely related to the degree of over-determinedness as defined by Roerink et al. (2000). The number of retained data points may be taken as a measure of the performance of the model. A disadvantage of HANTS is the lack of objective rules to determine its control parameters; parameterization requires experience and running several parameter combinations.

We used HANTS in two ways. First, long-term seasonal trends were determined for each pixel using the full GIMMS dataset (HA_{full}). Secondly, each year was analyzed separately (HA_{year}). Differences between the two filtered results were considered NDVI anomalies (A). Fig. 2 and Eq. (1) illustrate how the anomalies were calculated.

$$A(t) = HA_{year}(t) - HA_{full}(t) \quad (1)$$

Using anomalies, seasonality could be almost completely eliminated from the data, as demonstrated by the auto-correlation functions in Fig. 3. The algorithm was tuned to disregard values lower than zero that correspond to water or null-values in the GIMMS data. The eliminated values were replaced by *fills* — having a value of zero. The FET was set to 10% of the NDVI range (0.1). The number of iterations required depends on the biome and the length of the time-series. For a single-year analysis, 1 or 2 iterations are enough for all except some tropical areas in which the amplitude is limited and cloudiness affects even the fortnightly MVC images (Julien & Sobrino, 2010); in these cases a stable fit is obtained after 3 or 4 iterations. The i_{MAX} was fixed to 6 iterations in the yearly analysis. The full time-series is 26 times longer and it may need more iteration for a stable fit; for this reason the i_{MAX} was doubled to 12. The minimal number of retained data points was set to 16 and 416 for the yearly and the full datasets, respectively. This means that the output curve is always fitted to at least two-thirds of the original data points, even if the FET is not achieved. Table 1 lists the parameters used for analysis of both the full dataset and each year separately.

2.3. Extraction of phenological measures

Although satellite-observed phenology – also referred to as land surface phenology (LSP) – is not identical to plant phenology, it is considered to be related (Doktor et al., 2009; Liang & Schwartz, 2009; White et al., 2009). Therefore, LSP has been used to define developmental stages of vegetation. Analyzing trends in NDVI by vegetation development stage rather than by day-of-the-year eliminates variations in the start and length of the growing season — since the

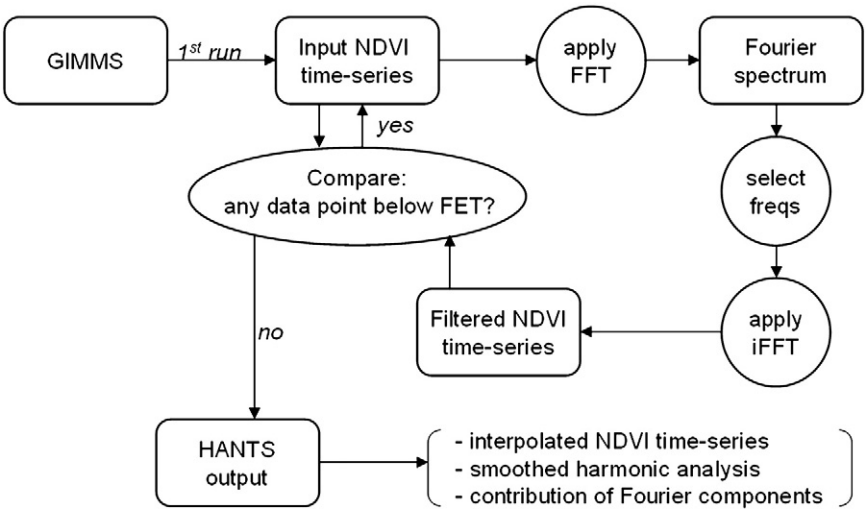

Fig. 1. Harmonic analysis of NDVI time-series flowchart.

growing season is fully contained within the first developmental stage (start of season, SoS), and the last stage (end of season, EoS). Various approaches have been described to derive SoS from NDVI time-series: half-maximum (White et al., 1997), 10% amplitude (Jönsson & Eklundh, 2002), inflection point (Moulin et al., 1997), maximum curvature (Zhang et al., 2003), delayed moving average and forward-looking moving average (Reed et al., 2003). Following White et al. (2009), we used the first derivative of the HANTS-smoothed NDVI profile, where SoS is defined as the maximum of the first derivative (maximum NDVI increase), and EoS is defined as the first time after SoS where the NDVI value drops below the value at the start of the growing season. Between SoS and EoS, ten equally spaced vegetation development stages were defined. This approach is reliable in comparison with several other methods (White et al., 2009), but it can be anticipated that the approach only works for single growing seasons and that it will not be able to detect multiple growing seasons. This limits the applicability of the method in multi-cropping regions. For illustration, Fig. 4 shows an example of a growing season in which several measures are indicated.

The NDVI values at each development stage ($NDVI_{ds}$) were calculated using the yearly harmonic fit (Eq. (2)), where *FC* represents the Fourier Component, $NDVI_{mean}$ is the mean NDVI (FC0), *A* is the amplitude, Φ is the phase shift and *x* is the day number represented in radians (Eq. (3)).

$$NDVI_{ds} = NDVI_{mean} + \sum_{i=FC_1}^{FC_{max}} A_i \cdot cos(i \cdot x + \Phi_i) \quad (2)$$

$$x = day / 365 \cdot 2\pi \quad (3)$$

For each growing season, this provided 12 $NDVI_{ds}$ values that were used as input for the seasonal Mann–Kendall (SMK) model.

2.4. Trend analysis

NDVI time-series are characterized by outliers, seasonality and serial auto-correlation. The GIMMS data were analyzed for trends using three different strategies that take account of these effects — all involving harmonic smoothing to remove outliers and seasonality.

The first approach – here referred to as the linear model (LM) – uses the smoothed time-series (624 fortnightly values from 1981 through 2006) to analyze anomalies (*A*) between the long-term harmonic fit and yearly fits (Eq. (1)). In the case of a perfectly stable seasonal pattern, without additional trend, there would be no anomalies; conversely, differences between the long-term and yearly fits may indicate

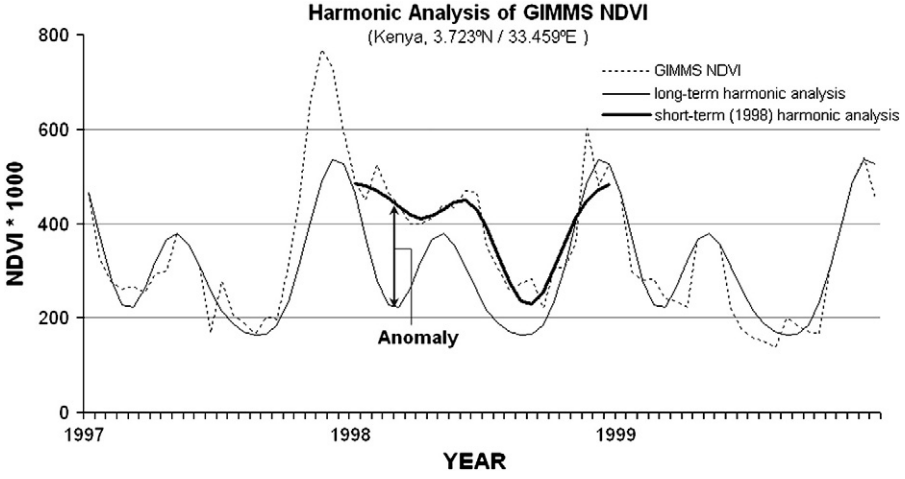

Fig. 2. Example of NDVI anomalies as derived from the long- and short-term fits of the harmonic analysis.

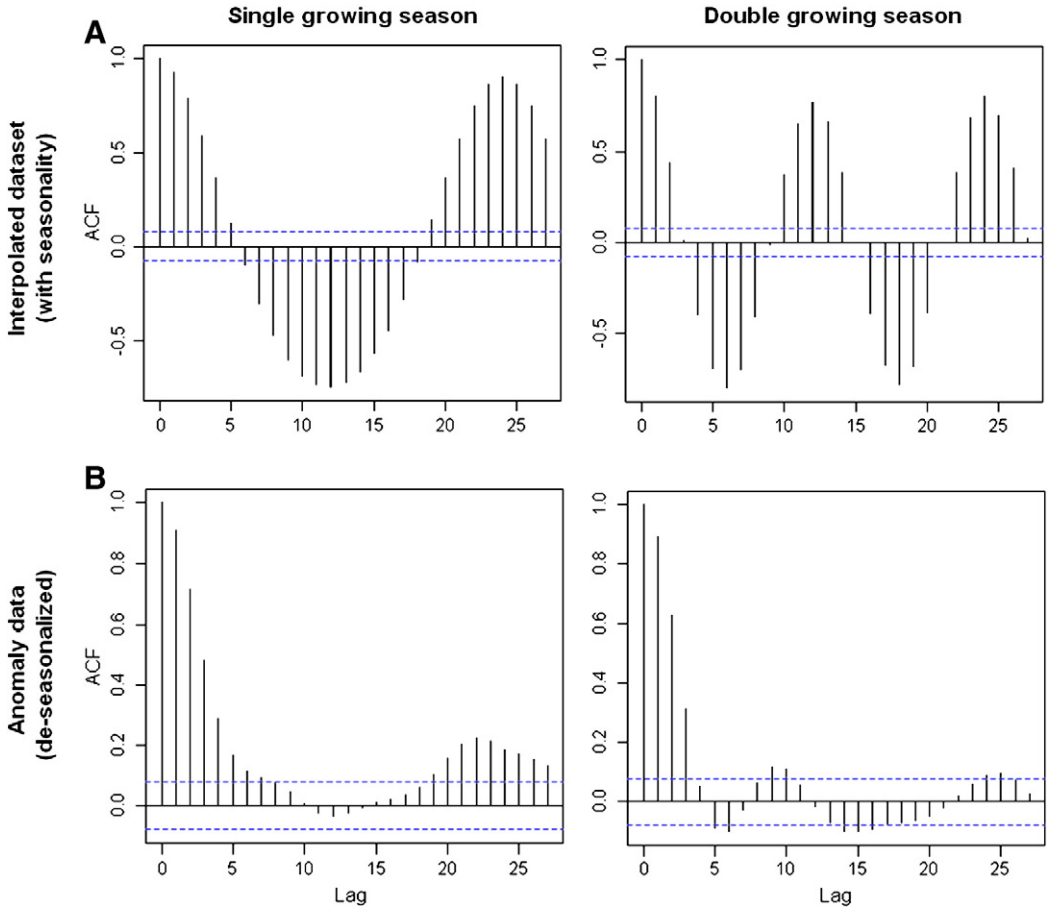

Fig. 3. Average auto-correlation functions (ACF) of GIMMS data (A: interpolated, B: anomalies) with fortnightly lags (lag 24 = 1 year). The dotted lines indicate the 95% confidence interval of zero auto-correlation. For both, single and double growing seasons, 30 pixels were used.

greening or browning, particularly if there is a significant negative or positive trend. Trends were quantified by the slope of the regression line derived from a linear model of the NDVI anomalies against time. The fitted slopes were tested for significance using analysis of variance (ANOVA) with a significance level (α) of 0.1. Only slopes that differ significantly from zero have been considered to indicate greening or browning trends.

The second approach used the HANTS-interpolated data without removing seasonality. This dataset would violate the assumption of independent *Y*-values, which is a basis for linear regression. For this reason, the non-parametric seasonal Mann–Kendall test was used. The test may be used with missing or tied data and its validity does not depend on the data being normally distributed. Mann (1945) first suggested using the Mann–Kendall test for significance of Kendall's τ for temporal trends and this approach has since been applied to seasonal data, mainly for hydrological analyses (Hirsch et al., 1982) and, more recently, with NDVI data (Alcaraz-Segura et al., 2009, 2010; Chamaille-Jammes et al., 2006; Pouliot et al., 2009). The test consists of computing the Kendall Score (S) and its variance separately for each season (p). In this case, p equals the number of observations in a year (24). For each season, n equals the number of observations in the record (26). S denotes the sign (sgn) of the change between subsequent samples and attains the value −1, 0 or +1 (Hirsch & Slack, 1984). These individual values are summed over all samples to obtain the seasonal statistic S_g (Eq. (4)). The sum over all seasons provides the final test statistic S' (Eq. (5)). Subsequently, the Kendall's rank correlation coefficient (τ) ranging between −1 and 1 (Kendall, 1938), is calculated (Eq. (6)). The null hypothesis H_0 is that for each of p seasons the n samples are randomly ordered (mean $S = 0$), versus the alternative hypothesis H_A of a monotonic trend in one or more seasons (Hirsch & Slack, 1984). H_0 was tested 2-sided against H_A and rejected when Kendall's τ of NDVI versus time is significantly different from zero ($\alpha = 0.1$). We then conclude that there *is* a monotonic trend in NDVI over time: a *greening trend* if $\tau > 0$ and a *browning trend* if $\tau < 0$.

$$S_g = \sum_{i<j} sgn\left(X_{jg} - X_{ig}\right) \quad g = 1, 2, \ldots, p \tag{4}$$

$$S' = \sum_{i=1}^{p} S_g \tag{5}$$

$$\tau = \frac{S'}{n(n-1)/2} \tag{6}$$

In a further step, the slope of this trend may be quantified using a Kendall slope estimator, but we preferred using the Kendall's rank correlation coefficient τ (Eq. (6)) directly.

Table 1
Parameters used in HANTS analysis.

	Single-year	Full GIMMS (26 years)
Number of data points	26	624
Fourier frequencies	0,1,2,3	0,26,52,78
Fit error tolerance (FET)	0.1	0.1
Max. iterations (i_{MAX})	6	12
Min. retained data points	16 (66.7%)	416 (66.7%)

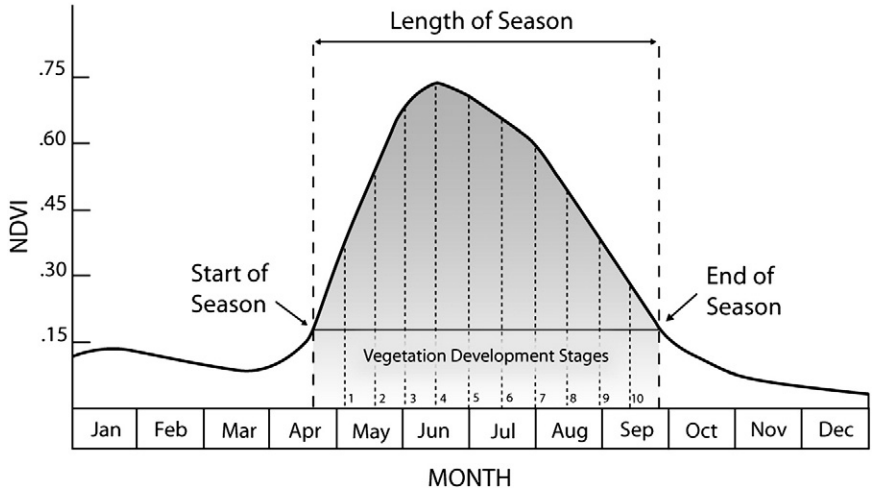

Fig. 4. Example of single growing season and related phenological measures. Start of season (SoS) is defined as the date of the inflexion point of the NDVI curve and end of season (EoS) as the date at which NDVI drops below the SoS value. In between these dates, 10 equally distanced vegetation development stages (VDS) are defined, covering the entire growing season (shaded area).

The seasonal approach compares events linked to the same seasonal phase (e.g. the first half of January); each scene is compared with the corresponding scene in other years but no cross-phase comparisons are made. In reality, phenological cycles vary in start and length according to the weather (Cleland et al., 2007; Moulin et al., 1997; Zhou et al., 2001); such variability may produce trends that may be falsely interpreted as greening or browning. Therefore, we propose a third method in which we use the SMK method to analyze trends by vegetation development stages (VDS) rather than by month or calendar day. This approach eliminates phenological shifts and variations in length of season (LoS). A linear model of yearly LoS values was used to find regions where greening or browning may be caused by a longer or shorter growing season, and the coefficient of variation (CoV) was used as a measure of reliability. A large variation in the identified LoS might indicate limitations to the model's capability to extract phenological parameters, for instance as a result of multiple growing seasons or low seasonal amplitude.

The International Geosphere–Biosphere Program (IGBP) global-land-cover-characteristics database (Loveland et al., 2000) was used to calculate statistics of our results according to biome. The 1 km dataset was re-sampled to 8 km resolution; the IGBP biome with the highest occurrence was then assigned to each pixel. To minimize edge-effects and mixed pixels, only clusters of more than 50 adjacent pixels belonging to the same IGBP class were used to calculate statistics.

3. Results

3.1. Linear trends in NDVI anomalies

Fig. 5a shows the results of the per-pixel linear trend analysis based on the anomaly dataset: green and red colors indicate greening and browning, respectively, and areas with little or no vegetation (yearly average NDVI<0.1) are masked. Overall, greening predominates, especially in the Northern Hemisphere and most notably in the boreal forests, eastern Europe, Asia Minor, the Sahel, and western India. In the southern hemisphere, greening is apparent in Western Australia and Botswana; and browning in the tropical Africa and Indonesia/Oceania and in northern Argentina.

3.2. Seasonal trends in interpolated NDVI

The SMK model reveals some of the same prominent regions of greening as the linear model, including western India and the Sahel, but it shows a different picture for some other regions; in some cases the detected trend is even inverted (e.g. parts of Botswana, Nigeria, Argentina and Australia). With only a few exceptions, the absolute Kendall τ scores were not larger than 0.25, which indicates rather weak trends and therefore, the map is not illustrated here.

The extent to which the SMK model is influenced by phenological variations is determined by the variation in SoS (phenological shift) and LoS (variation in length). If the growing season is stable, then the inter-annual VDS dates are close to each other — which is essential for the SMK model. Fig. 6 shows the variation in LoS using the slope of the linear trend (days/year) analysis and the CoV. It is clear that the extracted growing season is not stable everywhere: most regions show a positive or negative trend in LoS. This trend is significant ($\alpha = 0.1$) in parts of the Sahel, Asia, North-America and northern Europe, with lowest p-values in Sweden and Russia. The CoV values indicate that the extraction of LoS is stable (low CoV) across most of the northern hemisphere but less stable in the tropics and some parts of the southern hemisphere.

3.3. Seasonal trends in phenology-adjusted NDVI

The map of Kendall's τ scores from the VDS model (Fig. 5b) identifies the same areas of distinct greening but the absolute Kendall τ values are higher than those from the SMK model (commonly higher than 0.3 in areas with a greening or browning trend). Results from the VDS model should be interpreted in combination with the trend in LoS (Fig. 6) because greening can be caused either by a longer growing season or by a higher rate of production. The former effect is not captured by this method because the data were adjusted for changes in length of growing season.

3.4. Significance of trends

In Fig. 5, the non-masked pixels show significant trends ($\alpha = 0.1$), green indicates a positive trend and red a negative trend. The analysis of variance (ANOVA) of the LM results shows that the identified trends are significant in large parts of Europe, western India, Western Australia, the Sahel, Botswana and in some parts of Argentina, North America and Canada. Trends are weak in most tropical and tundra regions. The SMK model had non-significant values in most places and these results are not shown in Fig. 5; only few pixels with significant trends were found in western India, Western Australia and parts of the Sahel and Asia Minor. The VDS model was more powerful in rejecting the no-trend hypothesis: significant trends are revealed

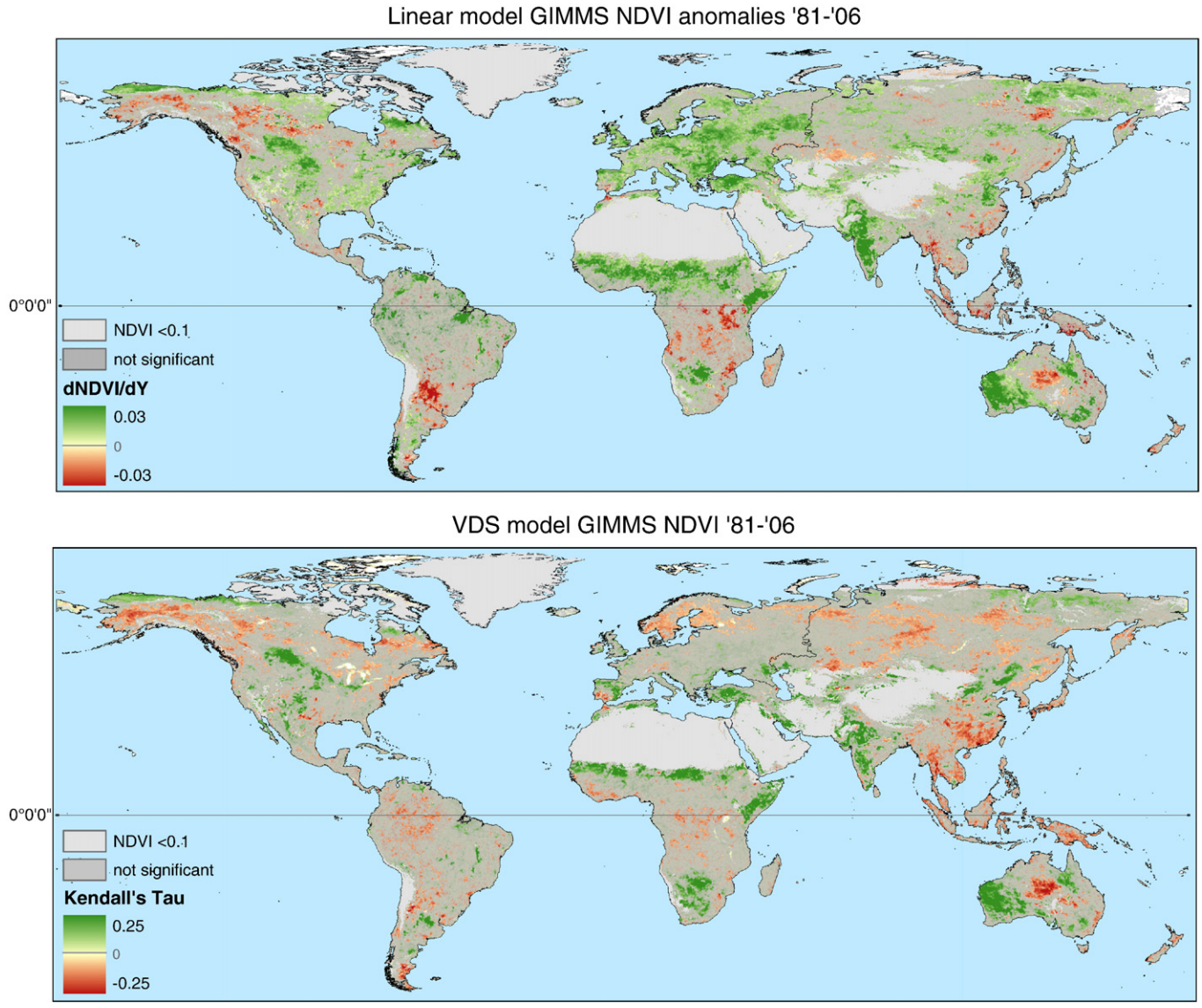

Fig. 5. (a) Trend in NDVI (dNDVI/dt, t in years), based on linear model of NDVI anomalies (1981–2006). (b) Kendall's tau from seasonal Mann–Kendall model on data adjusted by vegetation development stage (VDS). In both cases trends were assessed for significance using analysis of variance. Weak trends ($\alpha = 0.1$) have been masked.

in the northern Sahel, Asia Minor, Scandinavia, Western Australia and Botswana and smaller parts of western India, China, Canada and the Horn of Africa (Fig. 5b).

4. Discussion

4.1. Model results

The slopes found by the linear model using fortnightly NDVI values are very close to the linear trend analysis of yearly cumulative values published by Bai et al. (2008). On average, the absolute difference in trend is <0.001 units/year and never as much as 0.01 units/year — which supports the contention that reducing the temporal resolution to yearly values and the choice of annual break-point does not affect the trend slopes (Dent et al., 2009), given that the time-series start and end in the same phase.

The SMK model is valid only when it is conceptually correct to compare measurements based on calendar date. In case of NDVI time-series, this assumes that there is no phenological shift or variation in length of growing season throughout the measured period — which is not the case. Therefore, the SMK model identified only the most conspicuous greening regions; the likeliness (according to Kendall's τ) and significance (according to p-values) were generally low.

In the VDS model, Kendall's τ values were higher and p-values lower than in the SMK approach but VDS measures a different attribute of vegetation. The LM and SMK models use values with equal intervals (continuous fortnightly measurements) whereas VDS is based on an equal number of values for each growing season (the interval between these values might differ between years). Therefore, the VDS model does not show greening or browning associated with variation in growing season; it measures productivity within a growing season (changes in photosynthetic intensity) rather than of the total yearly productivity (changes in integrated NDVI).

4.2. Biome stratification

To summarize the model results by IGBP biomes: the LM indicates greening in all biomes except deciduous needle-leaved forest, where no trend is observed (Fig. 7A No. 3). Fig. 7B,E shows that the LoS trend opposes the photosynthetic intensity trend in all biomes except shrub land and savanna. For cropland, the LoS trend is negligible. In all forest types but especially in Scandinavian boreal forest, the VDS model indicates a decrease in photosynthetic intensity which is

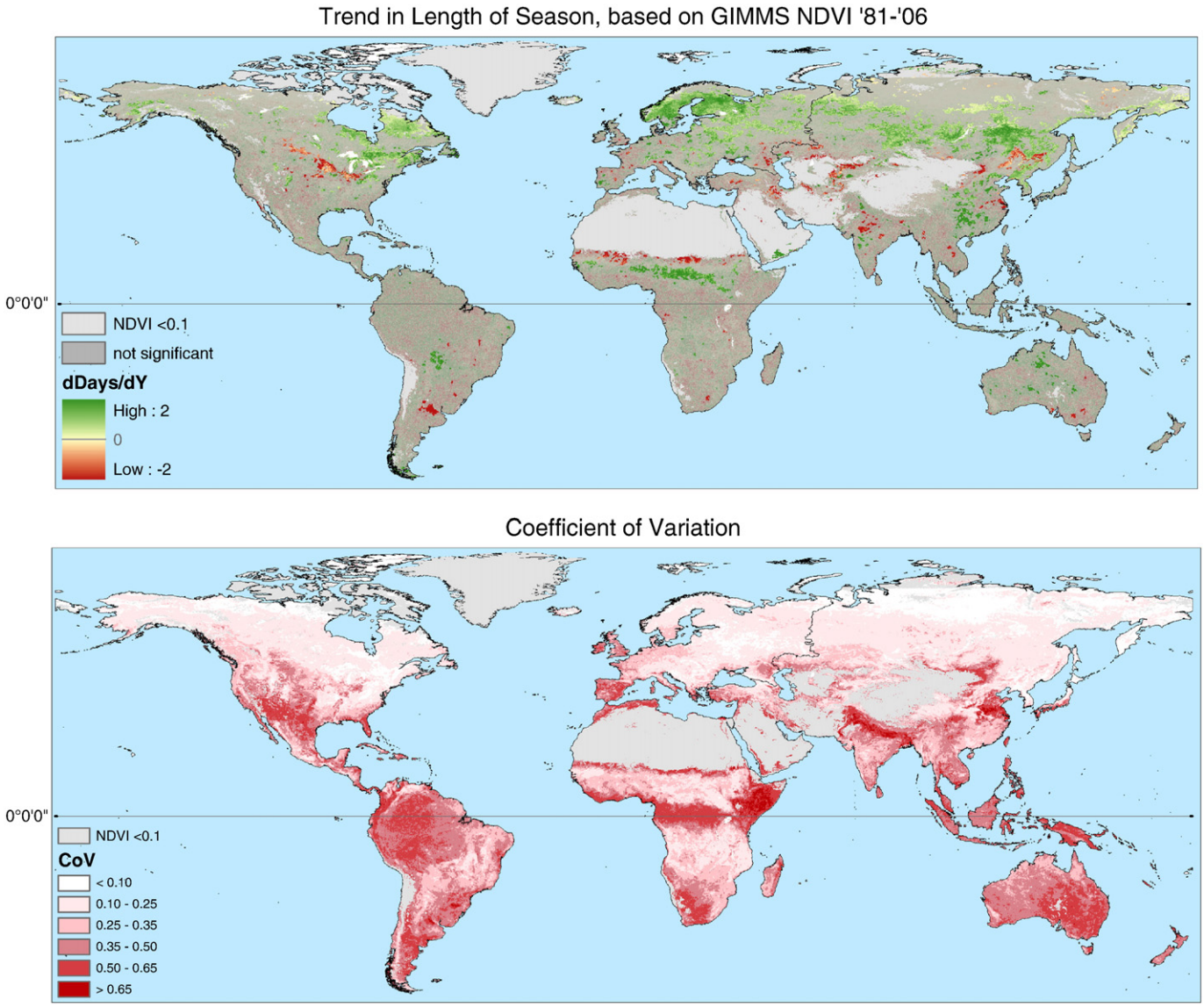

Fig. 6. Trend in length of growing season (LoS) derived from GIMMS using HANTS. (a) Slope of regression line: dLength/dt, Length in days, t in years. Weak trends ($\alpha = 0.1$) have been masked. (b) Coefficient of variation (CoV) of length of growing season (LoS).

counterbalanced by an overall increase in LoS (Figs. 5b and 6a). This might indicate that vegetation growth is no longer limited by temperature but by other limiting factors such as exhaustion of soil water or nutrients, which is in line with evapo-transpiration models (Zhang et al., 2009). On the other hand, the significance of the trends appears to be highest outside of the forest biomes (Fig. 7D) but, as already remarked, the power of the LM might be over-estimated (the predictive power of the models used and the performance of HANTS are discussed in Section 4.4).

4.3. Assessment of greening and browning trends

All three methods agreed on a significant greening across western India, Western Australia, Asia Minor, parts of the Sahel, Canada and the USA. However, even if field observations are available for validation, they are usually limited to a few points in time that may not be representative for 8 km pixels (Running & Nemani, 1988). We therefore compared our results with regional studies.

An inherent problem with time-series is that the initial status is often not known. The Sahel, for instance, experienced severe droughts in the late 1960s, 1970s and the early 1980s (Govaerts & Lattanzio, 2008; Nicholson, 2000; Zeng, 2003); recovery from these droughts shows as greening that is confirmed by several studies (Anyamba & Tucker, 2005; Herrmann et al., 2005; Heumann et al., 2007; Olsson et al., 2005) and there is controversy about whether this greening trend is concealing the role of human-induced land degradation (Hein & de Ridder, 2006; Prince et al., 2007). The VDS model shows strong positive trends in the northern parts of the Sahel, e.g. central Chad and northern Burkina Faso, which indicates that greening is caused by a more intense growing season rather than a longer season, in line with recovery from drought. Greening in the Deccan thorn forests of west India can be explained, in part, by recovery from degradation that occurred prior to the start of the GIMMS record (Champion & Seth, 1968); nowadays, parts of these shrub lands are protected (Chape et al., 2003) and recovering from human-induced degradation.

In Western Australia, Donohue et al. (2009) identified greening by an increase in fPAR (from AVHRR PAL) for the period 1981–2006; greening in north-eastern Australia is also in line with this increase in fPAR. In contrast, central Australia browned during this period, which might be explained by an 0.1 °C/year increase in temperature (Nemani et al., 2003). Also in the southern hemisphere, there has been greening in Botswana, which is in line with the 1% yearly increase in

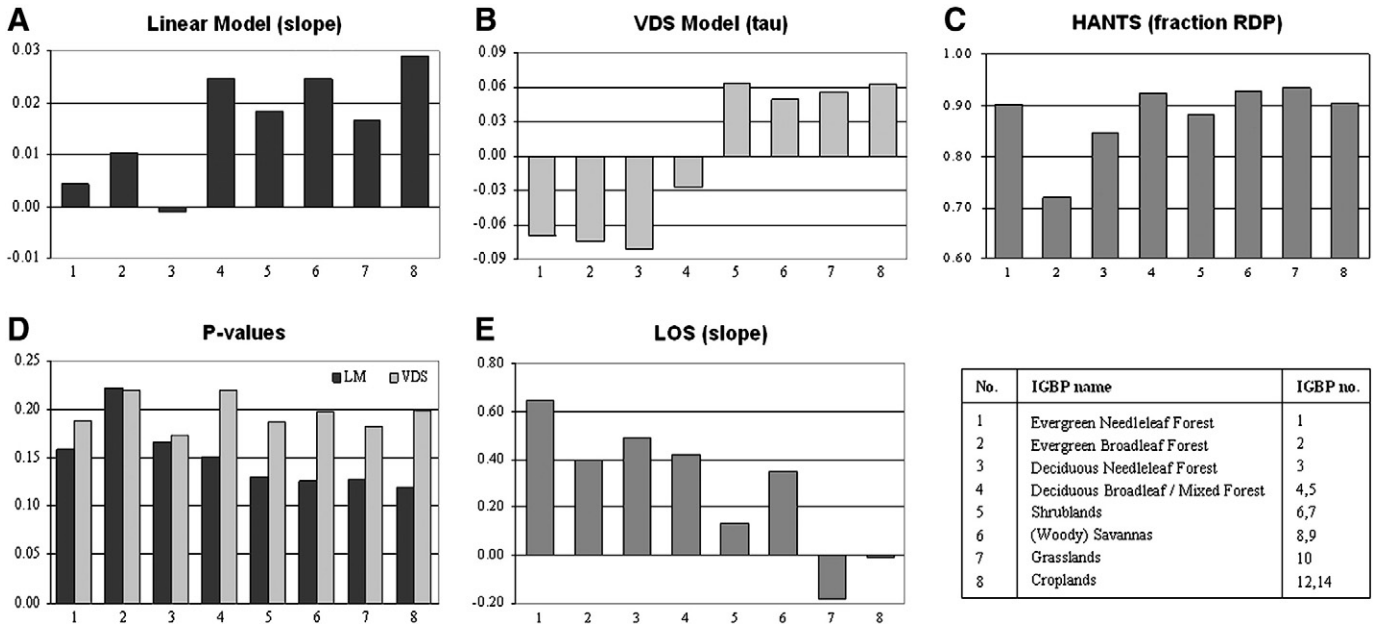

No.	IGBP name	IGBP no.
1	Evergreen Needleleaf Forest	1
2	Evergreen Broadleaf Forest	2
3	Deciduous Needleleaf Forest	3
4	Deciduous Broadleaf / Mixed Forest	4,5
5	Shrublands	6,7
6	(Woody) Savannas	8,9
7	Grasslands	10
8	Croplands	12,14

Fig. 7. statistics based on selected igbp biomes. (A) slope linear model, (B) Kendall's tau of vegetation development stage (vds) model, (C) fraction of retained data points (rdp) from hants model, (D) *p*-values from linear and vds models, (E) slope linear model length of season (los). Some igbp biomes have been merged based on similar responses. Biomes which are not shown are: urban, snow and ice, barren/sparsely vegetated, permanent wetlands and water bodies.

NPP found by Nemani et al. (2003) using AVHRR data in a production-efficiency model.

In Canada and the USA, all models show three notable greening regions: (1) the Low-Arctic tundra in Alaska, North West Territories and Yukon; (2) tundra and taiga east of Hudson's Bay; and (3) the prairie of southern Saskatchewan. These trends are most explicit in the VDS model and confirmed by other studies. Pouliot et al. (2009) used a similar Mann–Kendall approach with GIMMS data and found NDVI trends (of about 0.01 units/year) in all three regions. Goetz et al. (2005), using the same input data, confirm two out of three greening regions and, also, browning in Alaska, close to the British Columbia/Alberta border, and some parts of Quebec; they conclude that growth has increased in the tundra thanks to rising CO_2 concentration and temperature but, in the boreal forest, other factors including fire come into play. Alcaraz-Segura et al. (2009) also show that the GIMMS dataset largely misses greening due to post-fire recovery. This is also mentioned by Neigh et al. (2008) who attribute greening of the tundra to an increase in temperature and associated lengthening of the growing season; greening of the prairies is attributed mainly to an increase in rainfall, which has lead to much higher crop yields and conversion of more land to arable.

There is some discrepancy between trends in Eurasia. According to the linear model, greening prevails over browning, most conspicuously towards the east, in line with the relation between PAL NDVI and land surface temperature (Julien et al., 2006) — drier areas in the south have become hotter and even drier while northern Europe has become cooler. Stöckli and Vidale (2004) found a related positive trend in LoS of 1.4 days per year in central Europe (Germany) and a negative trend of −0.54 days per year in Scandinavia. Our harmonic analysis (Fig. 6) reproduced the 1.4 days trend for Germany (average of significant pixels) but shows an increase in LoS in Scandinavia of 1.47 days, which might indicate warming (Hüttich et al., 2007; Karlsen et al., 2007). The VDS model shows a decline in photosynthetic activity in Scandinavia and a longer growing season would explain this difference between the linear and the VDS model; greening due to a longer growing season does not necessarily produce a greater intensity of activity in the growing season.

In their global assessment and in detail in China, Bai and Dent (2009) and Bai et al. (2008) used GIMMS data in another way to assess land degradation and improvement, applying a linear model but introducing additional criteria of rain-use efficiency and energy-use efficiency to screen NDVI trends caused by drought and climatic warming. By translating NDVI to net primary productivity (NPP) using the relationship with MODIS NPP data, they derived a tangible measure of severity that can be subjected to economic appraisal. For China, they conclude that land degradation is most conspicuous in the rapidly-developing, humid south, rather than in the drylands of the north and west, where land reclamation initiatives have been concentrated. This conclusion is supported by our results from the LM and the VDS model.

4.4. Limitations and lessons learned

Harmonic analysis has removed some of the limitations of previous work that used only yearly-accumulated NDVI data. HANTS removes cloud interference and eliminates the influence of phenological shift between the northern and southern hemisphere — but does not affect inter-annual phenological shifts from which the LM and, especially, the SMK model suffer. This problem is solved by the single-growing-season normalization used in the VDS approach.

Serial auto-correlation remains an issue with the use of the linear model (Fig. 3); a significant deviation from the norm is likely to show for much of that growing season, rather than for a single measurement. Providing that seasonality is accounted for, the power of the statistical methods is mainly determined by the sample size; serial auto-correlation is an issue if the value of a sample is partly determined by its neighbors — so a dataset with serial auto-correlation contains less information than one of the same length with truly independent samples. Serial auto-correlation spuriously inflates the power of the test (McBride et al., 1994). It is a challenge to distinguish between *statistically significant changes* and *practically significant changes* and, in this sense, non-parametric models should be more robust than parametric models or, from a different perspective, the linear trend is more powerful in rejecting H_0 (Hirsch & Slack, 1984) — which explains why the LM trends appear more significant (Figs. 5 and 7D).

The performance of HANTS is biome-dependent. Most IGBP biomes show harmonic fits with more than 90% retained data points

(Fig. 7C) so the NDVI curve is fitted losing less than 10% of the original measurements. Exceptions are tropical evergreen broadleaf forest, deciduous needle-leaf forest, and shrub land. In the IGBP classification, the latter includes most tundra – where NDVI is zero, or a *fill* value, under snow cover and increases quickly to high values upon snowmelt (a situation that would be better described by double logistic fitting (Beck et al., 2006)). In the tropics, by contrast, NDVI is high throughout the year so noise in the phase-shift estimates makes it hard to extract phenological measures.

Better analysis requires a globally applicable method for deriving the start and length of growing season. This is neither simple nor straightforward (Hird & McDermid, 2009); with the HANTS technique used in this study, phenological measures can be derived automatically only for areas with a single annual growing season but it is essential to extract multi-season measures, for instance in eastern China, the Horn of Africa and the Ganges plain. For these regions, Fig. 6b shows a large coefficient of variation in the extracted LoS, probably caused by slight variations in the minimal NDVI between the growing seasons, which mean that, in one year, EoS occurs at the end of the first growing season and, in another year, at the end of the second season. This requires a procedure to extract multiple growth periods, e.g. Zhang et al. (2003), and, ideally, we should like one globally applicable method. Although several methods are available, each is suitable for only one or few biomes. The method proposed by Geerken (2009), defining a set of reference curves, is a step towards global application.

Applying NDVI trends for land degradation assessment, definition of land degradation remains contentious. Since the initial status is often not known, greening might represent recovery from drought or other disturbance; and greening resulting from the replacement of old-growth forest by crops or grassland might be considered as either degradation or land improvement, depending on the researchers point of view. In the humid tropics, the NDVI proxy is less reliable due to saturation of the signal (Myneni et al., 2002) and cloud cover; although most trends are in line with decreasing NPP (Nemani et al., 2003), there are also contradicting trends.

At present, choice of NDVI time-series presents a trade-off between temporal coverage and spatial resolution — between 10 years at 250–500 m resolution (MODIS) or almost 30 years at 1–8 km resolution (AVHRR). The longer period captures more climatic cycles and significant changes in land use and management, but a single pixel might contain several land use types or ecosystems. These data sets, however, are more suitable for capturing temporal dynamics. We have assessed monotonic trends in NDVI but vegetation trends are often complex and breaks or interruptions of trends are common (Angert et al., 2005; Slayback et al., 2003; Tucker et al., 2001; Verbesselt et al., 2010; Xin et al., 2008). Major volcanic eruptions can cause sudden breaks in a trend; fast-acting climatic cycles like El Niño or broad-scale land management practices may bring about large fluctuations. Gradual changes may be associated with slow-acting climatic cycles or the accumulation of changes in management but these gradual changes might, ultimately, trigger a catastrophic shift in the ecosystem (Scheffer et al., 2001). Trend breaks will become easier to identify as longer time-series of global observations become available.

5. Conclusions

We used harmonic analysis to enhance linear and monotonic trend analysis of GIMMS NDVI time-series data. Greening and browning trends are revealed but these cannot be quantified unambiguously. Variations in phenology confuse simple greening or browning trends but this aspect may be illuminated by using the seasonal Mann–Kendall (SMK) model with normalization of the growing season using vegetation development stages (VDS), rather than analysis by calendar day. The VDS model shows that greening or browning depends on growing intensity as much as yearly-aggregated NDVI.

At global scale, phenological shifts and variation in length of growing season render comparisons of NDVI values by calendar date unsatisfactory. However, it is difficult to extract phenological measures using a generalized method; the explaining power of the VDS model may be increased by, for instance, deriving these measures by several methods according to the phenology or climate zone, but this has yet to be undertaken.

Linear-model slopes derived from anomalies between long-term and yearly harmonic fits hardly differ from the slopes of yearly-aggregated NDVI data — so it unlikely that aggregating to yearly values severely influences NDVI trend analysis. However, the explaining power decreases with a decreasing number of observations.

All models were consistent in detecting a greening trend in western India, the Sahel and parts of Asia Minor, Canada, northern China and Western Australia; the biomes showing most-prominent greening were shrub land, savanna and cropland.

Acknowledgements

This work is partly financed through FAO contract PR35852. The authors thank Zhanguo Bai for providing data and results from previous studies. We appreciate the NASA GIMMS group providing the latest version of their NDVI data set. We also thank the reviewers for their helpful comments.

References

Alcaraz-Segura, D., Chuvieco, E., Epstein, H. E., Kasischke, E. S., & Trishchenko, A. (2009). Debating the greening vs. browning of the North American boreal forest: Differences between satellite datasets. *Global Change Biology*, *16*, 760—770.

Alcaraz-Segura, D., Liras, E., Tabik, S., Paruelo, J., & Cabello, J. (2010). Evaluating the consistency of the 1982–1999 NDVI trends in the Iberian Peninsula across four time-series derived from the AVHRR Sensor: LTDR, GIMMS, FASIR, and PAL-II. *Sensors*, *10*, 1291—1314.

Angert, A., Biraud, S., Bonfils, C., Henning, C. C., Buermann, W., Pinzon, J., et al. (2005). Drier summers cancel out the CO2 uptake enhancement induced by warmer springs. *Proceedings of the National Academy of Sciences of the United States of America*, *102*, 10823—10827.

Anyamba, A., & Tucker, C. J. (2005). Analysis of Sahelian vegetation dynamics using NOAA-AVHRR NDVI data from 1981–2003. *Journal of Arid Environments*, *63*, 596—614.

Bai, Z. G., & Dent, D. L. (2009). Recent land degradation and improvement in China. *AMBIO: A Journal of the Human Environment*, *38*, 150—156.

Bai, Z. G., Dent, D. L., Olsson, L., & Schaepman, M. E. (2008). Proxy global assessment of land degradation. *Soil Use and Management*, *24*, 223—234.

Baldocchi, D., Falge, E., Gu, L., Olson, R., Hollinger, D., Running, S., et al. (2001). FLUXNET: A new tool to study the temporal and spatial variability of ecosystem-scale carbon dioxide, water vapor, and energy flux densities. *Bulletin of the American Meteorological Society*, *82*, 2415—2434.

Barber, V. A., Juday, G. P., & Finney, B. P. (2000). Reduced growth of Alaskan white spruce in the twentieth century from temperature-induced drought stress. *Nature*, *405*, 668—673.

Beck, P. S. A., Atzberger, C., Høgda, K. A., Johansen, B., & Skidmore, A. K. (2006). Improved monitoring of vegetation dynamics at very high latitudes: A new method using MODIS NDVI. *Remote Sensing of Environment*, *100*, 321—334.

Cai, X. L., & Sharma, B. R. (2010). Integrating remote sensing, census and weather data for an assessment of rice yield, water consumption and water productivity in the Indo-Gangetic river basin. *Agricultural Water Management*, *97*, 309—316.

Chamaille-Jammes, S., Fritz, H., & Murindagomo, F. (2006). Spatial patterns of the NDVI-rainfall relationship at the seasonal and interannual time scales in an African savanna. *International Journal of Remote Sensing*, *27*, 5185—5200.

Champion, H. G., & Seth, S. K. (1968). *A revised survey of the forest types of India.* Delhi: Government of India Press.

Chape, S., Blyth, S., Fish, L., Fox, P., & Spalding, M. (2003). United Nations list of protected areas. *IUCN, Gland, Switzerland and UNEP-WCMC, Cambridge, UK* (pp. 44).

Cleland, E. E., Chuine, I., Menzel, A., Mooney, H. A., & Schwartz, M. D. (2007). Shifting plant phenology in response to global change. *Trends in Ecology & Evolution*, *22*, 357—365.

Cracknell, A. P. (2001). The exciting and totally unanticipated success of the AVHRR in applications for which it was never intended. *Advances in Space Research*, *28*, 233—240.

de Beurs, K. M., & Henebry, G. M. (2004). Trend analysis of the Pathfinder AVHRR Land (PAL) NDVI data for the deserts of central Asia. *Geoscience and Remote Sensing Letters, IEEE*, *1*, 282—286.

de Wit, A. J. W., & Su, B. (2005). Deriving phenological indicators from SPOT-VGT data using the HANTS algorithm. *2nd international SPOT-VEGETATION user conference* (pp. 195—201). Belgium: Antwerp.

Dent, D. L., Bai, Z. G., Schaepman, M. E., & Olsson, L. (2009). Response to Wessels: Comments on 'Proxy global assessment of land degradation'. *Soil Use and Management*, *25*, 93—97.

Doktor, D., Bondeau, A., Koslowski, D., & Badeck, F. -W. (2009). Influence of heterogeneous landscapes on computed green-up dates based on daily AVHRR NDVI observations. *Remote Sensing of Environment*, *113*, 2618—2632.

Donohue, R. J., McVicar, T. R., & Roderick, M. L. (2009). Climate-related trends in Australian vegetation cover as inferred from satellite observations, 1981–2006. *Global Change Biology*, *15*, 1025—1039.

Eklundh, L., & Olsson, L. (2003). Vegetation index trends for the African Sahel 1982–1999. *Geophysical Research Letters*, *30*, 1430.

Evans, J., & Geerken, R. (2004). Discrimination between climate and human-induced dryland degradation. *Journal of Arid Environments*, *57*, 535—554.

Foley, J. A., Levis, S., Costa, M. H., Cramer, W., & Pollard, D. (2000). Incorporating dynamic vegetation cover within global climate models. *Ecological Applications*, *10*, 1620—1632.

Geerken, R. A. (2009). An algorithm to classify and monitor seasonal variations in vegetation phenologies and their inter-annual change. *ISPRS Journal of Photogrammetry and Remote Sensing*, *64*, 422—431.

Goetz, S. J., Bunn, A. G., Fiske, G. J., & Houghton, R. A. (2005). Satellite-observed photosynthetic trends across boreal North America associated with climate and fire disturbance. *Proceedings of the National Academy of Sciences of the United States of America*, *102*, 13521—13525.

Goulden, M. L., Munger, J. W., Fan, S. -M., Daube, B. C., & Wofsy, S. C. (1996). Exchange of carbon dioxide by a deciduous forest: Response to interannual climate variability. *Science*, *271*, 1576—1578.

Govaerts, Y., & Lattanzio, A. (2008). Estimation of surface albedo increase during the eighties Sahel drought from Meteosat observations. *Global and Planetary Change*, *64*, 139—145.

Hein, L., & de Ridder, N. (2006). Desertification in the Sahel: A reinterpretation. *Global Change Biology*, *12*, 751—758.

Herrmann, S. M., Anyamba, A., & Tucker, C. J. (2005). Recent trends in vegetation dynamics in the African Sahel and their relationship to climate. *Global Environmental Change Part A*, *15*, 394—404.

Heumann, B. W., Seaquist, J. W., Eklundh, L., & Jönsson, P. (2007). AVHRR derived phenological change in the Sahel and Soudan, Africa, 1982–2005. *Remote Sensing of Environment*, *108*, 385—392.

Hird, J. N., & McDermid, G. J. (2009). Noise reduction of NDVI time series: An empirical comparison of selected techniques. *Remote Sensing of Environment*, *113*, 248—258.

Hirsch, R. M., & Slack, J. R. (1984). A nonparametric trend test for seasonal data with serial dependence. *Water Resources Research*, *20*, 727—732.

Hirsch, R. M., Slack, J. R., & Smith, R. A. (1982). Techniques of trend analysis for monthly water quality data. *Water Resources Research*, *18*, 107—121.

Holben, B. N. (1986). Characteristics of maximum-value composite images from temporal AVHRR data. *International Journal of Remote Sensing*, *7*, 1417—1434.

Hussian, M., Grimvall, A., Burdakov, O., & Sysoev, O. (2005). Monotonic regression for the detection of temporal trends in environmental quality data. *Match*, *54*, 535—550.

Hüttich, C., Herold, M., Schmullius, C., Egorov, V., & Bartalev, S. A. (2007). Indicators of Northern Eurasia's land-cover change trends from SPOT-VEGETATION time-series analysis 1998–2005. *International Journal of Remote Sensing*, *28*, 4199—4206.

IPCC (2007). Synthesis Report. *4th Assessment report of the intergovernmental panel on climate change* (pp. 52).

Jönsson, P., & Eklundh, L. (2002). Seasonality extraction by function fitting to time-series of satellite sensor data. *Geoscience and Remote Sensing, IEEE Transactions on*, *40*, 1824—1832.

Julien, Y., & Sobrino, J. A. (2010). Comparison of cloud-reconstruction methods for time series of composite NDVI data. *Remote Sensing of Environment*, *114*, 618—625.

Julien, Y., Sobrino, J. A., & Verhoef, W. (2006). Changes in land surface temperatures and NDVI values over Europe between 1982 and 1999. *Remote Sensing of Environment*, *103*, 43—55.

Karlsen, S. R., Solheim, I., Beck, P. S. A., Høgda, K. A., Wielgolaski, F. E., & Tommervik, H. (2007). Variability of the start of the growing season in Fennoscandia, 1982–2002. *International Journal of Biometeorology*, *51*, 513—524.

Kaufmann, R. K., Zhou, L., Knyazikhin, Y., Shabanov, V., Myneni, R. B., & Tucker, C. J. (2000). Effect of orbital drift and sensor changes on the time series of AVHRR vegetation index data. *IEEE Transactions on Geoscience and Remote Sensing*, *38*, 2584—2597.

Kendall, M. G. (1938). A new measure of rank correlation. *Biometrika*, *30*, 81—93.

Liang, L., & Schwartz, M. (2009). Landscape phenology: An integrative approach to seasonal vegetation dynamics. *Landscape Ecology*, *24*, 465—472.

Loveland, T. R., Reed, B. C., Brown, J. F., Ohlen, D. O., Zhu, Z., Yang, L., et al. (2000). Development of a global land cover characteristics database and IGBP DISCover from 1 km AVHRR data. *International Journal of Remote Sensing*, *21*, 1303—1330.

Lupo, F., Reginster, I., & Lambin, E. F. (2001). Monitoring land-cover changes in West Africa with SPOT Vegetation: Impact of natural disasters in 1998–1999. *International Journal of Remote Sensing*, *22*, 2633—2639.

Mann, H. B. (1945). Nonparametric tests against trend. *Econometrica*, *13*, 245—259.

McBride, G. B., Loftis, J. C., & Hamilton, N. Z. (1994). The most important statistical aspects. *Adriaanse. Proceedings of the International Workshop Monitoring Tailor-Made*. (pp. 153—161) The Netherlands: Beekbergen.

Menzel, A., Sparks, T. H., Estrella, N., Koch, E., Aasa, A., Ahas, R., et al. (2006). European phenological response to climate change matches the warming pattern. *Global Change Biology*, *12*, 1969—1976.

Metternicht, G., Zinck, J. A., Blanco, P. D., & Del Valle, H. F. (2010). Remote sensing of land degradation: Experiences from Latin America and the Caribbean. *Journal of Environmental Quality*, *39*, 42—61.

Moulin, S., Kergoat, L., Viovy, N., & Dedieu, G. (1997). Global-scale assessment of vegetation phenology using NOAA/AVHRR satellite measurements. *Journal of Climate*, *10*, 1154—1170.

Myneni, R. B., Hoffman, S., Knyazikhin, Y., Privette, J. L., Glassy, J., Tian, Y., et al. (2002). Global products of vegetation leaf area and fraction absorbed PAR from year one of MODIS data. *Remote Sensing of Environment*, *83*, 214—231.

Myneni, R. B., Keeling, C. D., Tucker, C. J., Asrar, G., & Nemani, R. R. (1997). Increased plant growth in the northern high latitudes from 1981 to 1991. *Nature*, *386*, 698—702.

Nagol, J. R., Vermote, E. F., & Prince, S. D. (2009). Effects of atmospheric variation on AVHRR NDVI data. *Remote Sensing of Environment*, *113*, 392—397.

Neigh, C. S. R., Tucker, C. J., & Townshend, J. R. G. (2008). North American vegetation dynamics observed with multi-resolution satellite data. *Remote Sensing of Environment*, *112*, 1749—1772.

Nemani, R. R., Keeling, C. D., Hashimoto, H., Jolly, W. M., Piper, S. C., Tucker, C. J., et al. (2003). Climate-driven increases in global terrestrial net primary production from 1982 to 1999. *Science*, *300*, 1560—1563.

Nicholson, S. (2000). Land surface processes and Sahel climate. *Reviews of Geophysics*, *38*, 117—138.

Olsson, L., Eklundh, L., & Ardö, J. (2005). A recent greening of the Sahel — trends, patterns and potential causes. *Journal of Arid Environments*, *63*, 556—566.

Pettorelli, N., Vik, J. O., Mysterud, A., Gaillard, J. -M., Tucker, C. J., & Stenseth, N. C. (2005). Using the satellite-derived NDVI to assess ecological responses to environmental change. *Trends in Ecology & Evolution*, *20*, 503—510.

Pouliot, D., Latifovic, R., & Olthof, I. (2009). Trends in vegetation NDVI from 1 km AVHRR data over Canada for the period 1985–2006. *International Journal of Remote Sensing*, *30*, 149—168.

Prince, S. D., & Tucker, C. J. (1986). Satellite remote sensing of rangelands in Botswana II. NOAA AVHRR and herbaceous vegetation. *International Journal of Remote Sensing*, *7*, 1555—1570.

Prince, S. D., Wessels, K. J., Tucker, C. J., & Nicholson, S. E. (2007). Desertification in the Sahel: A reinterpretation of a reinterpretation. *Global Change Biology*, *13*, 1308—1313.

Reed, B. C., White, M., & Brown, J. F. (2003). Remote sensing phenology. In M. D. Schwartz (Ed.), *Phenology: An Integrative Environmental Science* (pp. 365—381). Dordrecht, The Netherlands: Kluwer Academic Publishing.

Roerink, G. J., Menenti, M., & Verhoef, W. (2000). Reconstructing cloudfree NDVI composites using Fourier analysis of time series. *International Journal of Remote Sensing*, *21*, 1911—1917.

Rosenzweig, C., Casassa, G., Karoly, D. J., Imeson, A., Liu, C., Menzel, A., et al. (2007). Assessment of observed changes and responses in natural and managed systems. In M. L., O. F., J. P., P. J., & C. E. (Eds.), *Climate change 2007: Impacts, adaptation and vulnerability. contribution of working group II to the fourth assessment report of the intergovernmental panel on climate change* (pp. 79—131). Cambridge, UK: Cambridge University Press.

Running, S. W., & Nemani, R. R. (1988). Relating seasonal patterns of the AVHRR vegetation index to simulated photosynthesis and transpiration of forests in different climates. *Remote Sensing of Environment*, *24*, 347—367.

Scheffer, M., Carpenter, S., Foley, J. A., Folke, C., & Walker, B. (2001). Catastrophic shifts in ecosystems. *Nature*, *413*, 591—596.

Seaquist, J. W., Hickler, T., Eklundh, L., Ardö, J., & Heumann, B. W. (2008). Disentangling the effects of climate and people on Sahel vegetation dynamics. *Biogeosciences*, *6*, 469—477.

Sims, D. A., Rahman, A. F., Cordova, V. D., El-Masri, B. Z., Baldocchi, D. D., Bolstad, P. V., et al. (2008). A new model of gross primary productivity for North American ecosystems based solely on the enhanced vegetation index and land surface temperature from MODIS. *Remote Sensing of Environment*, *112*, 1633—1646.

Slayback, D. A., Pinzon, J. E., Los, S. O., & Tucker, C. J. (2003). Northern hemisphere photosynthetic trends 1982-99. *Global Change Biology*, *9*, 1—15.

Sparks, T. H., Aasa, A., Huber, K., & Wadsworth, R. (2009). Changes and patterns in biologically relevant temperatures in Europe 1941–2000. *Climate Research*, *39*, 191—207.

Stöckli, R., & Vidale, P. L. (2004). European plant phenology and climate as seen in a 20-year AVHRR land-surface parameter dataset. *International Journal of Remote Sensing*, *25*, 3303—3330.

Symeonakis, E., & Drake, N. (2004). Monitoring desertification and land degradation over sub-Saharan Africa. *International Journal of Remote Sensing*, *25*, 573—592.

Tottrup, C., & Rasmussen, M. S. (2004). Mapping long-term changes in savannah crop productivity in Senegal through trend analysis of time series of remote sensing data. *Agriculture, Ecosystems & Environments*, *103*, 545—560.

Tucker, C. J. (1979). Red and photographic infrared linear combinations for monitoring vegetation. *Remote Sensing of Environment*, *8*, 27—150.

Tucker, C. J., Pinzon, J. E., & Brown, M. E. (2004). *Global inventory modeling and mapping studies, NA94apr15b.n11-Vlg, 2.0*. College Park, Maryland: Global Land Cover Facility, University of Maryland.

Tucker, C., Pinzon, J., Brown, M., Slayback, D., Pak, E., Mahoney, R., et al. (2005). An extended AVHRR 8 km NDVI dataset compatible with MODIS and SPOT vegetation NDVI data. *International Journal of Remote Sensing*, *26*, 4485—4498.

Tucker, C. J., Slayback, D. A., Pinzon, J. E., Los, S. O., Myneni, R. B., & Taylor, M. G. (2001). Higher northern latitude normalized difference vegetation index and growing season trends from 1982 to 1999. *International Journal of Biometeorology*, *45*, 184—190.

Tucker, C. J., Vanpraet, C. L., Sharman, M. J., & Van Ittersum, G. (1985). Satellite remote sensing of total herbaceous biomass production in the senegalese sahel: 1980–1984. *Remote Sensing of Environment*, *17*, 233—249.

Verbesselt, J., Hyndman, R., Newnham, G., & Culvenor, D. (2010). Detecting trend and seasonal changes in satellite image time series. *Remote Sensing of Environment*, *114*, 106—115.

Wessels, K. J. (2009). Letter to the editor: comments on 'Proxy global assessment of land degradation'. *Soil Use and Management*, *25*, 91—92.
Wessels, K. J., Prince, S. D., Malherbe, J., Small, J., Frost, P. E., & VanZyl, D. (2007). Can human-induced land degradation be distinguished from the effects of rainfall variability? A case study in South Africa. *Journal of Arid Environments*, *68*, 271—297.
Westerling, A. L., Hidalgo, H. G., Cayan, D. R., & Swetnam, T. W. (2006). Warming and earlier spring increase western U.S. forest wildfire activity. *Science*, *313*, 940—943.
White, M. A., de Beurs, K. M., Didan, K., Inouye, D. W., Richardson, A. D., Jensen, O. P., et al. (2009). Intercomparison, interpretation, and assessment of spring phenology in North America estimated from remote sensing for 1982–2006. *Global Change Biology*, *15*, 2335—2359.
White, M. A., Running, S. W., & Thornton, P. E. (1999). The impact of growing-season length variability on carbon assimilation and evapotranspiration over 88 years in the eastern US deciduous forest. *International Journal of Biometeorology*, *42*, 139—145.
White, M. A., Thornton, P. E., & Running, S. W. (1997). A continental phenology model for monitoring vegetation responses to interannual climatic variability. *Global Biogeochemical Cycles*, *11*, 217—234.
Xin, Z., Xu, J., & Zheng, W. (2008). Spatiotemporal variations of vegetation cover on the Chinese Loess Plateau (1981—2006): Impacts of climate changes and human activities. *Science in China Series D: Earth Sciences*, *51*, 67—78.
Yu, D., Shi, P., Shao, H., Zhu, W., & Pan, Y. (2009). Modelling net primary productivity of terrestrial ecosystems in East Asia based on an improved CASA ecosystem model. *International Journal of Remote Sensing*, *30*, 4851—4866.
Zeng, N. (2003). Drought in the Sahel. *Science*, *302*, 999—1000.
Zhang, X., Friedl, M. A., Schaaf, C. B., Strahler, A. H., Hodges, J. C. F., Gao, F., et al. (2003). Monitoring vegetation phenology using MODIS. *Remote Sensing of Environment*, *84*, 471—475.
Zhang, K., Kimball, J. S., Mu, Q., Jones, L. A., Goetz, S. J., & Running, S. W. (2009). Satellite based analysis of northern ET trends and associated changes in the regional water balance from 1983 to 2005. *Journal of Hydrology*, *379*, 92—110.
Zhou, L., Tucker, C. J., Kaufmann, R. K., Slayback, D. A., Shabanov, N. V., & Myneni, R. B. (2001). Variations in northern vegetation activity inferred from satellite data of vegetation index during 1981 to 1999. *Journal of Geophysical Research*, *106*, 20269—20283.
Zika, M., & Erb, K. H. (2009). The global loss of net primary production resulting from human-induced soil degradation in drylands. *Ecological Economics*, *69*, 310—318.